

# Ginzburg-Landau Analysis for the Antiferromagnetic Order in the Fulde-Ferrell-Larkin-Ovchinnikov Superconductor

Youichi YANASE<sup>1,2\*</sup> and Manfred Sigrist<sup>2</sup>

<sup>1</sup>*Department of Physics, Niigata University, Ikarashi, Niigata 950-2181, Japan*

<sup>2</sup>*Theoretische Physik, ETH-Honggerberg, 8093 Zurich, Switzerland*

(Received Today 2011)

Antiferromagnetic (AFM) order in the Fulde-Ferrell-Larkin-Ovchinnikov (FFLO) superconducting state is analyzed on the basis of the Ginzburg-Landau theory. To examine the possible AFM-FFLO state in a heavy fermion superconductor CeCoIn<sub>5</sub>, we focus on the incommensurate AFM order characterized by the wave vector  $\vec{Q} = \vec{Q}_0 \pm \vec{q}_{\text{inc}}$  with  $\vec{Q}_0 = (\pi, \pi, \pi)$  and  $\vec{q}_{\text{inc}} \parallel [110]$  or  $[1\bar{1}0]$  in the tetragonal crystal structure. We formulate the two component Ginzburg-Landau model to discuss two degenerate incommensurate AFM states with  $\vec{q}_{\text{inc}} \parallel [110]$  and  $[1\bar{1}0]$ . Owing to the broken translation symmetry in the FFLO state, multiple phase diagram of single-q phase and double-q phase is obtained under the magnetic field along  $[100]$  or  $[010]$ . Magnetic properties in each phase are investigated and compared with the neutron scattering and nuclear magnetic resonance (NMR) measurements. An ultrasonic measurement is proposed for a future experimental study on the possible AFM-FFLO state in CeCoIn<sub>5</sub>. The field orientation dependence of the AFM order in CeCoIn<sub>5</sub> is discussed.

KEYWORDS: FFLO superconductivity, unconventional magnetism, CeCoIn<sub>5</sub>

## 1. Introduction

More than 40 years ago, Fulde and Ferrell,<sup>1)</sup> and Larkin and Ovchinnikov<sup>2)</sup> proposed the appearance of a spatially modulated phase in a spin polarized superconductor. The original BCS theory is based on a condensate of Cooper pairs with vanishing total momentum. On the other hand, this Fulde-Ferrell-Larkin-Ovchinnikov (FFLO) phase is composed of Cooper pairs with finite momentum. A spontaneous breaking of spatial symmetry is implied by the internal degrees of freedom of the FFLO phase arising from inversion or reflection symmetry.

The search for the FFLO phase has been pursued since its proposal with mixed success. Indeed it has been discussed for various systems such as superconductors,<sup>3-9)</sup> cold atom gases,<sup>10-12)</sup> and quark matter.<sup>13)</sup> Nevertheless, the discovery of a new superconducting phase in CeCoIn<sub>5</sub> at high magnetic fields and low temperatures<sup>3,4)</sup> came as a surprise and triggered much interest, as it satisfied all the immediate criteria for an FFLO state, sitting in the right parameter space in the  $H$ - $T$ -phase diagram.<sup>14)</sup>

The high-field superconducting (HFSC) phase of CeCoIn<sub>5</sub> has been examined based on the FFLO-concepts by many groups.<sup>14-23)</sup> Recent observations of magnetic order coexisting with the HFSC phase point towards a more complex situation and demands the reexamination and extension of the basic picture.<sup>24,25)</sup> Neutron scattering measurements show that the wave vector of AFM order is incommensurate,  $\vec{Q} = \vec{Q}_0 \pm \vec{q}_{\text{inc}}$  with  $\vec{Q}_0 = (\pi, \pi, \pi)$  and  $\vec{q}_{\text{inc}} \sim (0.12\pi, \pm 0.12\pi, 0)$ , and independent of the orientation of inplane magnetic field.<sup>25,26)</sup> The ordered Ce-moments  $\vec{M}_{\text{AF}}$  are oriented along the  $c$ -axis. For the magnetic field along  $[110]$ ,  $\vec{q}_{\text{inc}}$  is perpendicular to the applied magnetic field  $\vec{q}_{\text{inc}} \sim (0.12\pi, -0.12\pi, 0)$ . The data for the magnetic field along  $[100]$  direction may be best interpreted as being due to

two degenerate incommensurate AFM states with  $\vec{q}_{\text{inc}} \sim (0.12\pi, 0.12\pi, 0)$  and  $\vec{q}_{\text{inc}} \sim (0.12\pi, -0.12\pi, 0)$ ,<sup>25,26)</sup> as we will discuss below.

We may conclude that this magnetic order is stabilized by superconductivity because it is absent in the normal state. This strong cooperation between the magnetism and superconductivity contrasts the behavior of other heavy fermion superconductors where the magnetic order competes usually with superconductivity.<sup>27)</sup> It is worth noting that the HFSC phase is enlarged by pressure.<sup>19)</sup> This feature is also different from the other magnetic phase diagram in Ce-based heavy fermion systems.<sup>27)</sup>

The observation of this unconventional magnetic order initiated a number of attempts for theoretical explanations.<sup>28-36)</sup> Here we propose a theory based on the presence of an AFM quantum critical point near the superconducting phase of CeCoIn<sub>5</sub>.<sup>37-41)</sup> As we have shown previously, AFM order appears within the inhomogeneous Larkin-Ovchinnikov state in the vicinity of the AFM quantum critical point.<sup>28,29)</sup> The mechanism coupling magnetism and FFLO superconductivity is consistent with the fact that the magnetic order is restricted to the superconducting phase in the  $H$ - $T$  phase diagram.<sup>24,25)</sup> Alternative proposals are based on the emergence of a pair density wave state together with magnetic order in the HFSC phase.<sup>34-36)</sup>

In order to identify the HFSC phase of CeCoIn<sub>5</sub> it is important to find unambiguous ways to compare the proposed phase with experimental findings. Here we intend to examine the AFM-FFLO state proposed by us previously. First, we show that several phases can appear in the AFM-FFLO state when the magnetic field is applied along  $[100]$  or  $[010]$  direction. Second, we clarify the magnetic structure of each phases and discuss the consistency with the experimental results of CeCoIn<sub>5</sub>.

## 2. Ginzburg-Landau theory

Our theoretical analysis is based on a phenomenological Ginzburg-Landau model formulated on the basis of the microscopic calculation in Refs. 29 and 42. and motivated by recent neutron scattering measurements of Kenzelmann *et al.*<sup>25,26</sup> We describe the AFM order in the inhomogeneous Larkin-Ovchinnikov state by means of the Ginzburg-Landau functional of the free energy,

$$\begin{aligned} \frac{F(\eta_1, \eta_2)}{F_0} = & [(T/T_N^0 - 1) + \xi_{\text{AF}}^2(\vec{q}_1 - \vec{q}_{\text{inc}}^{(1)})^2]\eta_1^2 \\ & + [(T/T_N^0 - 1) + \xi_{\text{AF}}^2(\vec{q}_2 - \vec{q}_{\text{inc}}^{(2)})^2]\eta_2^2 \\ & + \frac{1}{2}(\eta_1^2 + \eta_2^2)^2 + b\eta_1^2\eta_2^2 \\ & + c_1 H_x H_y (\eta_1^2 - \eta_2^2) \\ & - \frac{1}{2}\eta_1\eta_2 \sum_n c_2(n)\delta(\vec{q}_1 - \vec{q}_2, 2n\vec{q}_{\text{FFLO}}). \quad (1) \end{aligned}$$

We use an order parameter with two components,  $\eta_1$  and  $\eta_2$  corresponding to the two degenerate AFM states with  $\vec{Q} \sim \vec{Q}_0 \pm \vec{q}_{\text{inc}}^{(1)}$  and  $\vec{Q} \sim \vec{Q}_0 \pm \vec{q}_{\text{inc}}^{(2)}$ . The wave vectors of incommensurate AFM state in the system with full translational symmetry are given by  $\vec{q}_{\text{inc}}^{(1)} = (0.125\pi, 0.125\pi, 0)$  and  $\vec{q}_{\text{inc}}^{(2)} = (-0.125\pi, 0.125\pi, 0)$ . In our study the incommensurate wave vectors  $\vec{q}_{\text{inc}}^{(1)}$  and  $\vec{q}_{\text{inc}}^{(2)}$  are not microscopically derived but assumed on the basis of the experimental results in Refs. 25 and 26. We think that the  $\vec{q}_{\text{inc}}^{(1)}$  and  $\vec{q}_{\text{inc}}^{(2)}$  are pinned through nesting features in the band structures. Note that the order parameter  $(\eta_1, \eta_2)$  is not a vector, but a director.

We describe the magnetic moment  $M(\vec{r}) = e^{i\vec{Q}_0 \cdot \vec{r}} M_{\text{AF}}(\vec{r})$  where  $M_{\text{AF}}(\vec{r})$  is a slowly varying amplitude of the magnetic moment perpendicular to the applied magnetic field at  $\vec{r} = (x, y, z)$ . Then, the AFM staggered moment is given by

$$M_{\text{AF}}(\vec{r}) = M_0[\eta_1 \cos(\vec{q}_1 \cdot \vec{r}) + \eta_2 \cos(\vec{q}_2 \cdot \vec{r})]. \quad (2)$$

Both  $M_0$  and  $F_0$  are scaling factors to write the Ginzburg-Landau free energy in a dimensionless form (eq.(1)). Moreover,  $T_N^0$  is the "bare" Néel temperature (for  $c_1 = c_2(n) = 0$ , i.e. unrenormalized by coupling to the magnetic field and to the FFLO-modulation of the superconducting phase), and  $\xi_{\text{AF}}$  is the correlation length of the AFM order. The inplane lattice constant is chosen as the unit length.

Choosing the coupling constant  $b$  positive we stabilize the "single- $q$ " magnetic structure  $(\eta_1, \eta_2) \propto (1, 0)$  or  $(0, 1)$ , while a negative value for  $b$  would favor the "double- $q$ " magnetic structure  $(\eta_1, \eta_2) \propto (1, 1)$ . From the microscopic point of view  $b > 0$  is more appropriate, since the single- $q$  magnetic phase gains more condensation energy than the double- $q$  phase in most cases. We assume  $b > 0$  in this paper, while the cases of negative  $b$  have been discussed in Ref. 43.

The constant  $c_1$  denotes the coupling strength of the order parameter to the external magnetic field  $\vec{H} = (H_x, H_y, H_z)$ . Comparing with the neutron scattering data for  $\vec{H} \parallel [110]$ ,<sup>25</sup>  $c_1$  must be positive in CeCoIn<sub>5</sub>,

as to pick the incommensurate wave vector  $\vec{q}_{\text{inc}}^{(2)} \perp [1\bar{1}0]$ . This choice is consistent with our theoretical analysis for the AFM-FFLO state,<sup>28,29,42</sup> while it is incompatible with the theoretical scenario without taking the FFLO state into account.<sup>32,33</sup> When we consider the magnetic field along the [100] (or [010]) direction, this term is inactive and, therefore, the degeneracy of  $\eta_1$  and  $\eta_2$  remains. We focus on this situation in this paper.

The effects of the broken translational symmetry in the inhomogeneous Larkin-Ovchinnikov state are taken into account in the last term (commensurate term) of eq.(1). We define  $\delta(\vec{q}_1 - \vec{q}_2, 2n\vec{q}_{\text{FFLO}}) = 1$  when the commensurate condition  $\vec{q}_1 - \vec{q}_2 = 2n\vec{q}_{\text{FFLO}}$  is satisfied for an integer  $n$  and otherwise  $\delta(\vec{q}_1 - \vec{q}_2, 2n\vec{q}_{\text{FFLO}}) = 0$ . The modulation vector of FFLO state is denoted as  $\vec{q}_{\text{FFLO}}$ , and then the order parameter of superconductivity is described as  $\Delta(\vec{r}) = \Delta_0 \sin(\vec{q}_{\text{FFLO}} \cdot \vec{r})$ . The commensurate term describes the pinning effect of FFLO nodal planes for the AFM moment. According to the microscopic calculation based on the Bogoliubov-de-Gennes (BdG) equation, the AFM moment is enhanced around the FFLO nodal planes where the superconducting order parameter vanishes.<sup>28,29,42</sup> Then, we obtain the positive coupling constant  $c_2(n) \geq 0$ .

## 3. Phase Diagram

Let us now consider the FFLO state in a case with  $2n\vec{q}_{\text{FFLO}}$  is close to  $\vec{q}_{\text{inc}}^{(1)} - \vec{q}_{\text{inc}}^{(2)}$  for one integer  $n = N$ , i.e. we assume  $\vec{q}_{\text{inc}}^{(1)} - \vec{q}_{\text{inc}}^{(2)} \sim 2N\vec{q}_{\text{FFLO}}$ . This has consequences for the structure of the magnetic order. When the wave vector  $\vec{q}_{\text{inc}}^{(1)} - \vec{q}_{\text{inc}}^{(2)}$  is not in the vicinity of  $2n\vec{q}_{\text{FFLO}}$  for any integer  $n$ , the single- $q$  magnetic phase with  $(\eta_1, \eta_2) \propto (1, 0)$  or  $(0, 1)$  is realized.

We determine the magnetic structure by minimizing the Ginzburg-Landau free energy (eq.(1)) with respect to the order parameters  $\eta_1$  and  $\eta_2$  and their momentum  $\vec{q}_1$  and  $\vec{q}_2$  for given temperature  $T$  and FFLO wave vector  $\vec{q}_{\text{FFLO}}$ . We assume  $\eta_1 \geq \eta_2 \geq 0$  without loss of the generality. As for the direction of  $\vec{q}_{\text{FFLO}}$ , we assume  $\vec{q}_{\text{FFLO}} = q_{\text{FFLO}}\hat{x}$  for  $\vec{H} \parallel [100]$  as in Refs. 29 and 42. Then, the phase diagram is determined by the renormalized parameters  $T/T_N^0$  and  $\xi_{\text{AF}}q_0$ , where  $q_0$  is defined by  $\vec{q}_{\text{inc}}^{(1)} - \vec{q}_{\text{inc}}^{(2)} + 2q_0\hat{x} = 2N\vec{q}_{\text{FFLO}}$ . The parameter  $q_0$  describes the mismatch of the harmonic FFLO wave vector  $2N\vec{q}_{\text{FFLO}}$  and the incommensurability along the  $\hat{x}$ -axis  $\vec{q}_{\text{inc}}^{(1)} - \vec{q}_{\text{inc}}^{(2)}$ . Note that  $q_0 = 0$  when the condition  $\vec{q}_{\text{inc}}^{(1)} - \vec{q}_{\text{inc}}^{(2)} = 2N\vec{q}_{\text{FFLO}}$  is satisfied. Since the FFLO wave number  $q_{\text{FFLO}}$  grows with increasing magnetic field and/or decreasing temperature,<sup>14</sup>  $q_0$  increases with the magnetic field, and changes its sign at the line in the  $H$ - $T$  phase diagram.

We find two possible phases. One is the single- $q$  phase where

$$\eta_1 > \eta_2, \quad (3)$$

$$\vec{q}_1 = \vec{q}_{\text{inc}}^{(1)} + (1-x)q_0\hat{x}, \quad (4)$$

$$\vec{q}_2 = \vec{q}_{\text{inc}}^{(2)} - (1+x)q_0\hat{x}. \quad (5)$$

Note that  $x$  lies between 0 and 1 and is determined by

minimizing the free energy. The other is the double- $q$  phase where

$$\eta_1 = \eta_2, \quad (6)$$

$$\vec{q}_1 = \vec{q}_{\text{inc}}^{(1)} + q_0 \hat{x}, \quad (7)$$

$$\vec{q}_2 = \vec{q}_{\text{inc}}^{(2)} - q_0 \hat{x}. \quad (8)$$

By analyzing the quadratic terms of eq.(1), we find that the double- $q$  phase is stabilized immediately below the Néel temperature for  $(\xi_{\text{AF}}q_0)^2 \leq c_2(N)/8$ , while a single- $q$  phase is stabilized for  $(\xi_{\text{AF}}q_0)^2 > c_2(N)/8$ .

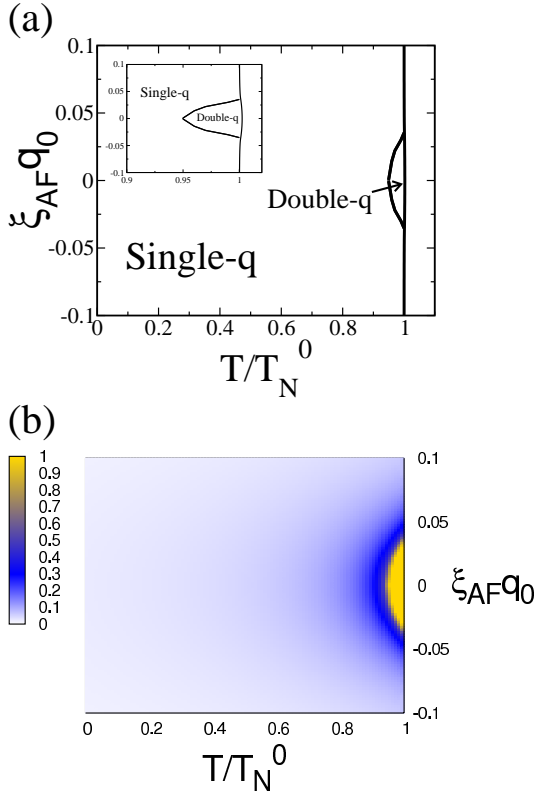


Fig. 1. (Color online) (a) Phase diagram of Ginzburg-Landau model in eq.(1) for  $\xi_{\text{AF}}q_0$  and the renormalized temperature  $T/T_N^0$ . The definition of  $q_0$  is given in the text. The  $q_0$  increases with the magnetic field. The inset shows the same phase diagram scaled up around the Néel temperature. (b) The ratio of order parameters  $\eta_2/\eta_1$ .

Figure 1(a) shows the phase diagram obtained by the numerical minimization of the free energy in eq.(1) using the parameters  $b = 0.1$  and  $c_2(N) = 0.01$ . The single- $q$  phase is stable in most parameter regimes, because the quartic term  $b\eta_1^2\eta_2^2$  dominates. Only near the Néel temperature quadratic terms are leading and can stabilize the double- $q$  phase for small  $|\xi_{\text{AF}}q_0| \leq \sqrt{c_2(N)/8}$ . As shown in the inset of Fig. 1(a), the Néel temperature increases slightly around the commensurate line  $\xi_{\text{AF}}q_0 = 0$  due to the locking-in effect of the magnetic and the FFLO modulation. However, the enhancement of the Néel temperature  $T_N - T_N^0 = \frac{c_2(N)}{4}T_N^0$  is rather small, unless the coupling constant  $c_2(N)$  is large. Various phase diagrams for several parameter sets ( $b, c(N)$ ) have been shown in

Ref. 43. We here focus on the case of Fig. 1 and examine the consistency with experiments.

Figure 1(b) shows the ratio of order parameters  $\eta_1$  and  $\eta_2$ . We find that  $\eta_2/\eta_1 = 1$  in the double- $q$  phase while the ratio decreases in the single- $q$  phase with decreasing temperature  $T/T_N^0$  and/or increasing the mismatch  $|\xi_{\text{AF}}q_0|$ .

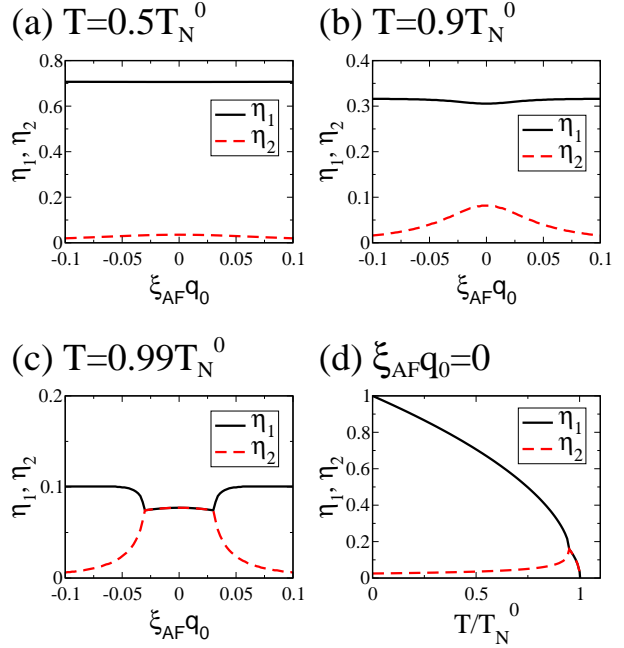


Fig. 2. (Color online) The  $\xi_{\text{AF}}q_0$  dependences of order parameters  $\eta_1$  and  $\eta_2$  at (a)  $T = 0.5T_N^0$ , (b)  $T = 0.9T_N^0$ , and (c)  $T = 0.99T_N^0$ , respectively. (d) Temperature dependence of  $\eta_1$  and  $\eta_2$  at  $\xi_{\text{AF}}q_0 = 0$ .

The behavior of the order parameter can be seen in the plot of the  $\xi_{\text{AF}}q_0$  dependence of order parameters for  $T = 0.5T_N^0$ ,  $T = 0.9T_N^0$ , and  $T = 0.99T_N^0$  in Figs. 2(a)-2(c), respectively while the temperature dependence for  $\xi_{\text{AF}}q_0 = 0$  is shown in Fig. 2(d). The phase transition between the double- $q$  phase and single- $q$  phase is a continuous second-order transition. This phase transition is characterized by the broken mirror symmetry with respect to the  $x$ - and  $y$ -axes in the single- $q$  phase.

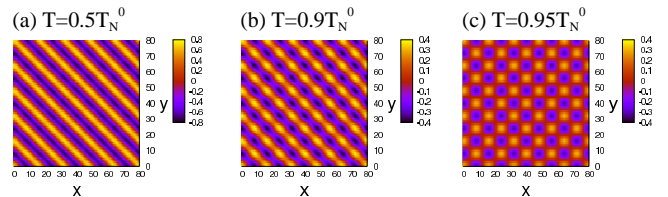


Fig. 3. (Color online) The spatial dependences of AFM staggered moment  $M_{\text{AF}}(\vec{r})$  at  $\vec{r} = (x, y, 0)$ . (a) Single- $q$  phase at  $T = 0.5T_N^0$ , (b) Single- $q$  phase at  $T = 0.9T_N^0$ , and (c) Double- $q$  phase at  $T = 0.95T_N^0$ , respectively. We choose  $\xi_{\text{AF}}q_0 = 0$ .

We show the spatial dependences of the AFM staggered moment  $M_{\text{AF}}(\vec{r})$  for several parameters in Fig. 3.

Since the AFM moment is uniform along the  $z$ -direction, we show the  $M_{\text{AF}}(\vec{r})$  in the  $x$ - $y$  plane. The checkerboard magnetic structure is realized in the double- $q$  phase (Fig. 3(c)), while it changes to the stripe magnetic structure in the single- $q$  phase (Figs. 3(a) and 3(b)). We investigate these phases in more details and discuss the experimental results of CeCoIn<sub>5</sub> in the next section.

#### 4. HFSC Phase in CeCoIn<sub>5</sub>

In order to discuss the possible AFM-FFLO states in CeCoIn<sub>5</sub> on the basis of our Ginzburg-Landau analysis, we show the schematic phase diagram of CeCoIn<sub>5</sub> for the magnetic field and temperature in Fig. 4. The amplitude of FFLO modulation vector  $q_{\text{FFLO}}$  has a maximal possible value of  $q_{\text{FFLO}} \sim 1/\xi$  with  $\xi$  being the coherence length of the superconducting state. According to the experimental estimate of  $\xi$ , the minimum number of  $N$ , which satisfies the condition  $\vec{q}_{\text{inc}}^{(1)} - \vec{q}_{\text{inc}}^{(2)} = 2N\vec{q}_{\text{FFLO}}$  for commensurate wave vectors, is approximately  $N \sim 4$ . This condition is satisfied in the FFLO state on a sequence of commensurate lines (dashed lines in Fig. 4) with  $N = 4, 5, 6, 7, \dots$ , and the double- $q$  phase is stabilized around the AFM transition line (shaded area of Fig. 4). Note that the double- $q$  phase does not appear close to the first-order normal-to-FFLO transition line at which the AFM moment as well as the superconducting order parameter appear discontinuously. Since the coupling constant  $c_2(N)$  decreases with increasing  $N$ , the double- $q$  phase is suppressed in the low magnetic field region.

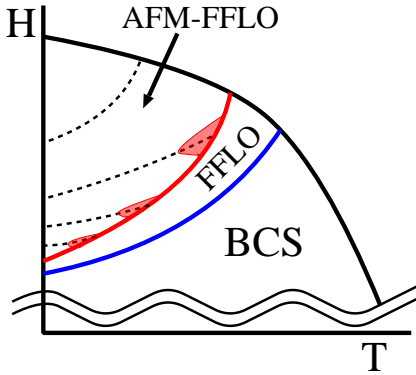


Fig. 4. (Color online) Schematic phase diagram for the magnetic field along [100] direction. “BCS”, “FFLO”, and “AFM-FFLO” states are shown in the figure. The dashed lines show the commensurate lines which are explained in the text. The shaded region shows the double- $q$  phase in the AFM-FFLO state.

It should be noticed that the AFM-FFLO phase is mostly covered by the single- $q$  phase. Therefore, the experimental results of CeCoIn<sub>5</sub> should be compared with the properties of the single- $q$  phase. There are ways to distinguish the single- $q$  phase experimentally from the double- $q$  phase. Indeed the experimental results are consistent with the single- $q$  phase, as we will discuss below.

When we take into account the broken translational symmetry arising from the vortex lattice, other commensurate

lines can appear in the phase diagram and stabilize the double- $q$  phase around  $T = T_N$ . However, it is expected that the effect of the vortex lattice on the magnetic order is smaller than that of the FFLO nodal planes when the Maki parameter is large enough to make the lattice spacing of vortices much larger than the coherence length.

##### 4.1 Neutron scattering

The neutron scattering measurements have well determined the structure of AFM order and its magnetic field dependence.<sup>25,26</sup> For the magnetic field along [100] direction the elastic Bragg peaks appear at both  $\vec{Q} = \vec{Q}_0 \pm \vec{q}_{\text{inc}}^{(1)}$  and the symmetry related  $\vec{Q} = \vec{Q}_0 \pm \vec{q}_{\text{inc}}^{(2)}$ .<sup>25,26</sup> At first sight, this result seems to be incompatible with the single- $q$  phase in which, for instance, the Bragg peaks at  $\vec{Q} = \vec{Q}_0 \pm \vec{q}_{\text{inc}}^{(2)}$  should be much weaker than those at  $\vec{Q} = \vec{Q}_0 \pm \vec{q}_{\text{inc}}^{(1)}$  (see Fig. 5(a)). However, taking into account that the sets of wave vectors correspond to degenerate single- $q$  phases in a field along [100], it is rather likely that the domains have formed of the two states  $|\eta_1| > |\eta_2|$  and  $|\eta_1| < |\eta_2|$ . Because the domain structure is history-dependent, it can be identified in future experiments, for example, by changing the field orientation slightly away from [100] direction in order to lift the degeneracy.

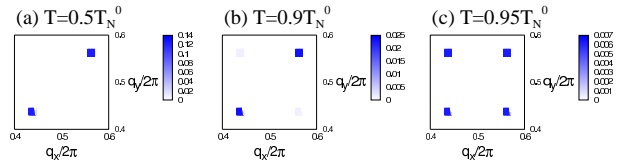


Fig. 5. (Color online) The weight of Bragg peaks defined by  $|M(\vec{q})|^2$  with  $M(\vec{q}) = \frac{1}{N_0} \sum_{\vec{r}} M(\vec{r}) e^{i\vec{q}\cdot\vec{r}}$  and  $\vec{q} = (q_x, q_y, \pi)$ . The summation  $\sum_{\vec{r}}$  is taken over the  $N_0$  lattice sites. (a) Single- $q$  phase at  $T = 0.5T_N^0$ , (b) Single- $q$  phase at  $T = 0.9T_N^0$ , and (c) Double- $q$  phase at  $T = 0.95T_N^0$ , respectively. We choose  $\xi_{\text{AF}}q_0 = 0$ .

As discussed above and stated in eqs.(4), (5), (7) and (8), the incommensurate wave vectors  $\vec{q}_1$  and  $\vec{q}_2$  depend on the magnetic field. However, the deviation from  $\vec{q}_{\text{inc}}^{(1)}$  is rather small for the main Bragg peak, with  $|\vec{q}_1 - \vec{q}_{\text{inc}}^{(1)}| \leq \xi_{\text{AF}}^{-1} \sqrt{c_2(N)}/8$ . For the parameters  $c_2(N) = 0.01$  and  $\xi_{\text{AF}} = 3$ , we obtain  $|\vec{q}_1 - \vec{q}_{\text{inc}}^{(1)}| < 0.004\pi$ . Moreover, the shift of  $\vec{q}_1$  rapidly decreases upon lowering the temperature below  $T_N$  (see Fig. 6). Therefore, additionally challenged by the tininess of the magnetic moment near the Néel temperature, most likely the shift of Bragg peaks is experimentally unobservable. Indeed, in the experiments no magnetic field dependence of  $\vec{q}_1$  has been observed so far.<sup>25,26</sup> Nevertheless, it would be interesting to search for a possible shift of  $\vec{q}_1$  in future experiments.

Finally, we would like to state that also the case of  $b < 0$  stabilizing the double- $q$  phase shows four Bragg peaks consistent with the neutron scattering data for  $\vec{H} \parallel [100]$  without having to assume domain formation.

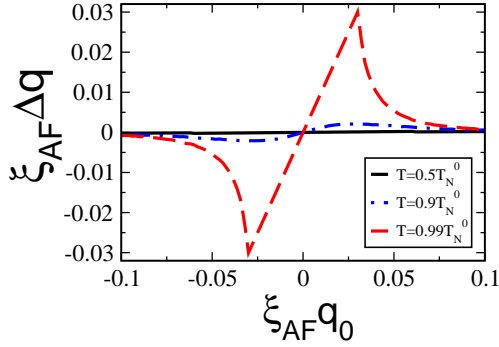


Fig. 6. (Color online) The shift of the position of main Bragg peak from  $\vec{q}_{inc}^{(1)}$ . We plot  $\xi_{AF}\Delta q$  for  $T = 0.5T_N^0$ ,  $T = 0.9T_N^0$ , and  $T = 0.99T_N^0$ , where  $\Delta q$  is defined by  $\Delta q\hat{x} = \vec{q}_1 - \vec{q}_{inc}^{(1)}$ .

However, this case yields a sizable shift of  $\vec{q}_1$  at low temperature, and therefore seems to be incompatible with the neutron scattering data.<sup>43)</sup> Moreover, as we will elucidate now this scenario is incompatible with the NMR measurements.

#### 4.2 NMR

The first evidence for AFM order in the HFSC phase of CeCoIn<sub>5</sub> has been obtained by the NMR measurement.<sup>24)</sup> The analysis of the NMR spectrum pointed towards incommensurate AFM order. This interpretation has subsequently been confirmed by the neutron scattering measurements in a decisive way.<sup>25,26)</sup> Recent analysis showed that the direction of AFM moment along *c*-axis is also consistent with the NMR data by assuming dipolar hyperfine coupling.<sup>44–47)</sup>

Applying the magnetic field parallel to the *x*-axis there are three distinct In-sites for NMR, the inplane In(1)-site and the out-of-plane In(2a)- and In(2b)-site. The latter two lie on *yz*- and *zx*-planes, respectively, relative to the Ce-layers. Looking at the dipolar fields due to the magnetic moments on the Ce-sites only the In(2b)-site develops a field component parallel to the *x*-axis which contributes to the Knight shift. Restricting to the two nearest Ce-ions of a In(2b)-site at  $\vec{r}$  we obtain for the dipolar field,

$$H_x(\vec{r}) = A[M(\vec{r} + \vec{b}_+) - M(\vec{r} + \vec{b}_-)], \quad (9)$$

with  $A$  a constant and  $\vec{b}_\pm = (\pm 1/2, 0, c')$  with  $c'$  the distance of In(2b) site from the Ce-plane. Note that there are In(2b)-sites above and below the Ce-plane. Using eq.(2) we derive,

$$H_x(\vec{r}) = A'M_0 \cos(\vec{Q}_0 \cdot \vec{r}) [\eta_1 \cos(\vec{q}_1 \cdot \vec{r}) + \eta_2 \cos(\vec{q}_2 \cdot \vec{r})], \quad (10)$$

which eventually leads to the field distribution  $P(h)$  observable in the Knight shift,

$$P(h) = \frac{1}{N_0} \sum_{\vec{r}} \delta(h - H_x(\vec{r})). \quad (11)$$

The sum runs over  $N_0$  sites of square lattice representing the In(2b)-sites.

It is obvious that  $P(h)$  shows a broad distributions

with two peaks at the upper and lower edge of the distribution, if  $(\eta_1, \eta_2) \propto (1, 0)$  or  $(0, 1)$  (single-*q* phase as in Fig. 7(a)). A single peak in the center of the distribution ( $h = 0$ ) is found for  $|\eta_1| = |\eta_2|$  (double-*q* phase as in Fig. 7(c)). In Fig. 7 we show the evolution of the distribution function  $P(h)$  for the same parameters as used for Figs. 3(a-c).

The experimentally observed Knight shift distribution has the shape of a broad double peak structure. This is consistent with the realization of a single-*q* phase and clearly does not fit to the double-*q* phase. Thus, the phase diagram with the AFM-FFLO state, which is almost entirely covered by the single-*q* phase, is consistent with the actual NMR measurements.

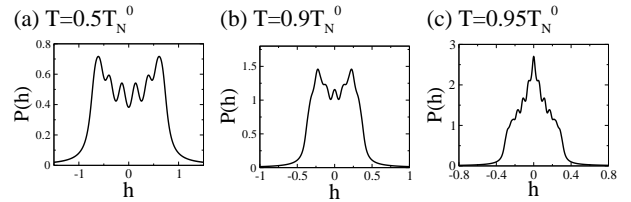


Fig. 7. The distribution function of the internal field  $P(h)$  at the In(2b) sites given by eq.(11). The parameters are the same as in Figs. 3(a), 3(b) and 3(c), respectively. We choose  $AM_0 = \frac{1}{2}$ .

We now turn to the relationship between the analysis given in this paper and our previous microscopic study of the spatial structure of AFM-FFLO state. We have shown that three basic forms of the AFM-FFLO state are possible.<sup>42)</sup> We distinguish (1) the 'extended' case for which the magnetic moments are slightly suppressed around the nodal planes of FFLO-superconducting order parameter, (2) the 'weakly localized' case in which the magnetic moments are slightly enhanced around the nodal planes, and (3) the 'strongly localized' case with a magnetic order parameter very localized around the nodal planes. Our phenomenological theory in this paper is justified in the cases (1) and (2), while it is invalid for the case (3) because the incommensurate wave vector  $\vec{q}_{inc}$  would not be parallel to  $[110]$  and  $[1\bar{1}0]$  for the magnetic field along  $[100]$  axis. According to our analysis, only the case (2) is consistent with the neutron scattering measurements in which the position of magnetic Bragg peaks is independent of the magnetic field and  $\vec{q}_{inc}$  is perpendicular to the field ( $\vec{q}_{inc} \perp \vec{H}$ ) for  $\vec{H} \parallel [110]$  or  $\vec{H} \parallel [1\bar{1}0]$ .<sup>25,26)</sup>

In the case (2), a weak enhancement of magnetic moment around the FFLO nodal planes, which is not taken into account in this paper, affects the NMR spectrum. This results in tails at the edges of the distribution function  $P(h)$ . This additional contribution to  $P(h)$  does, however, not alter the qualitative feature of the double peak structure anticipated for the single-*q* phase.

We here discuss the NMR measurements at In(1)- and In(2a)-sites. Since the AFM moment does not (or only weakly) yield internal field at these sites, we may avoid the effect of AFM order and elucidate the magnetic properties of FFLO state without AFM order. Recent

NMR measurement at In(1)- and In(2a)-sites actually reports an evidence for the FFLO superconducting state in CeCoIn<sub>5</sub>.<sup>47)</sup>

### 4.3 Ultrasonic measurement

As we have shown in Fig. 4, the region of the AFM-FFLO state of CeCoIn<sub>5</sub> is dominantly the single- $q$  phase. Because the order of single- $q$  phase has  $Z_2$  character, a probe sensitive to the crystal symmetry could give further helpful evidence for this phase. Ultrasound measurements provide such an experimental tool, as we discuss here.

AFM order and crystal lattice deformations are coupled to each other through the band structure and spin-orbit coupling. Avoiding microscopic details, we may describe this interplay by means of a general Ginzburg-Landau free energy,

$$F' = F(\eta_1, \eta_2) + F_{\text{el-af}} + F_{\text{el}}, \quad (12)$$

$$F_{\text{el-af}} = \{\gamma_1(\epsilon_{xx} + \epsilon_{yy}) + \gamma_2\epsilon_{zz}\}(\eta_1^2 + \eta_2^2) + \gamma_3\epsilon_{xy}(\eta_1^2 - \eta_2^2), \quad (13)$$

$$F_{\text{el}} = \frac{1}{2}[C_{11}(\epsilon_{xx}^2 + \epsilon_{yy}^2) + C_{33}\epsilon_{zz}^2 + 2C_{12}\epsilon_{xx}\epsilon_{yy} + 2C_{13}(\epsilon_{xx} + \epsilon_{yy})\epsilon_{zz} + 4C_{44}(\epsilon_{yz}^2 + \epsilon_{zx}^2) + 4C_{66}\epsilon_{xy}^2], \quad (14)$$

where the coefficients  $C_{ij}$  represent elastic constants of a tetragonal crystal lattice, and  $\epsilon_{ij} = \frac{1}{2}(\partial u_i/\partial x_j + \partial u_j/\partial x_i)$  defines the strain tensor with  $\vec{u}$  being the local displacement vector.  $\gamma_i$  are coupling constants between strain and magnetic order parameter.

We examine now the coupling to ultrasound modes, longitudinal (L) and transversal (T1, T2) with inplane and  $c$ -axis propagation directions. For the propagation along [100] the following strain fields are involved,

$$\text{L: } \epsilon_{xx}, \quad \text{T1: } \epsilon_{xy}, \quad \text{T2: } \epsilon_{xz}, \quad (15)$$

while for [110],

$$\text{L: } \epsilon_{xx} = \epsilon_{yy} = \epsilon_{xy}, \quad \text{T1: } \epsilon_{xx} = -\epsilon_{yy}, \quad \text{T2: } \epsilon_{xz} = \epsilon_{yz}, \quad (16)$$

and for [001],

$$\text{L: } \epsilon_{zz}, \quad \text{T: } \epsilon_{xz}, \epsilon_{yz}. \quad (17)$$

Note that for T1 (T2) the transverse polarization lies in the basal plane (along the  $z$ -axis) and for T it has two independent polarization directions in the basal plane.

The sound velocity corresponding to these modes can be renormalized at the phase transition to the AFM-FFLO phase. This corresponds to the renormalization of the elastic constants, given by

$$\tilde{C}_{\alpha\beta} = \frac{d^2 F'}{d\epsilon_\alpha d\epsilon_\beta} = C_{\alpha\beta} + \sum_{n=1,2} \frac{\partial^2 F'}{\partial \epsilon_\alpha \partial \eta_n} \frac{\partial \eta_n}{\partial \epsilon_\beta}, \quad (18)$$

at equilibrium, i.e.

$$\frac{\partial F'}{\partial \eta_n} = \frac{\partial F'}{\partial \epsilon_\alpha} = 0. \quad (19)$$

We find coupling to the ultrasound mode, if the corre-

Table I. Coupling of ultrasound modes to single- and double- $q$  phases: "yes" or "no" denote which elastic constants are renormalized or unrenormalized.

mode	single- $q$	double- $q$	$C_{ij}$
<b>[100]</b>			
L	yes	yes	$C_{11}$
T1	yes	yes	$C_{66}$
T2	no	no	$C_{44}$
<b>[110]</b>			
L	yes	yes	$C_{11} + C_{12} + 2C_{66}$
T1	no	no	$C_{11} - C_{12}$
T2	no	no	$C_{44}$
<b>[001]</b>			
L	yes	yes	$C_{33}$
T	no	no	$C_{44}$

Table II. Anomaly of ultrasonic sound mode at the magnetic transition. The sound velocity (and elastic constant) shows a "kink", "jump", or "divergence". In case of the double transition, magnetic transition to the double- $q$  state occurs at  $T = T_N$  and that to the single- $q$  state occurs at  $T = T_{N2}$ . In case of the single transition, the transition to the single- $q$  state occurs at  $T = T_N$ .

mode	double transition		single transition
	$T = T_N$	$T = T_{N2}$	$T = T_N$
T1 for [100]	kink	divergence	jump
L for all	jump	jump	jump

sponding terms,

$$\left. \frac{\partial^2 F_{\text{el-af}}}{\partial \epsilon_\alpha \partial \eta_n} \right|_{\epsilon_\alpha=0; \eta_n=\eta_{n0}}, \quad (20)$$

are finite. We give now a list of couplings for the two phases, single- $q$  [ $(\eta_1, \eta_2) \propto (1, 0)$ ] and double- $q$  [ $(\eta_1, \eta_2) \propto (1, 1)$ ].

Table I shows that both single- and double- $q$  phases couple in the same pattern to the different modes. Thus there are no selection rules distinguishing the two phases. Important is, however, to notice that both phases couple not only to longitudinal modes, but also to a transverse (T1) mode propagating in the [100] direction. This is a signature of the multi-component (magnetic) order parameter, since a single component magnetic order, such as the commensurate AFM order with  $\vec{Q} = \vec{Q}_0$ , does not couple to any transverse mode. The anomaly in the T1 mode arises from the last term of eq.(13) which is described as  $\gamma_3\epsilon_{xy}Q_{xy}$  with use of the quadrupole order parameter  $Q_{xy} = \eta_1^2 - \eta_2^2$ . Thus, the internal degree of freedom having a quadrupole symmetry manifests itself in the transverse sound mode, as in the non-magnetic quadrupole order appearing in many heavy fermion systems.<sup>48)</sup>

We find characteristic behaviors of this sound mode and summarize in Table II. For  $|\xi_{\text{AF}q_0}| \leq \sqrt{c_2(N)}/8$  the double magnetic transitions occur at  $T = T_N$  and  $T = T_{N2}$  ( $T_{N2} < T_N$ ). Then, the T1 sound mode propagating along [100] direction shows a kink at  $T = T_N$  and diverges at  $T = T_{N2}$ . On the other hand, when the single magnetic transition to the single- $q$  phase occurs for  $|\xi_{\text{AF}q_0}| \geq \sqrt{c_2(N)}/8$ , this sound mode shows a jump

at  $T = T_N$ . Thus, these two cases can be distinguished by the ultrasonic measurement for the T1 mode along [100] direction. All longitudinal modes show a jump at the magnetic phase transition.

The ultrasonic measurement by Watanabe *et al.* actually found the anomaly in the T1 mode along [100] direction, but it has been attributed to the modulation of superconducting order parameter in the FFLO state.<sup>15)</sup> More detailed ultrasonic measurement with focus on the AFM order is highly desired to identify the HFSC phase of CeCoIn<sub>5</sub>.

It is obvious from eq.(13) that a uniaxial stress along [110] or  $[\bar{1}\bar{1}0]$  direction ( $\epsilon_{xy} \neq 0$ ) would split the degeneracy between  $\eta_1$  and  $\eta_2$  such that a single domain phase could be obtained for the single- $q$  phase.

## 5. Summary and Discussion

In this study we investigated the coexistence of the incommensurate AFM order with the FFLO superconducting state to interpret the properties of the HFSC phase of CeCoIn<sub>5</sub>. We assume that two incommensurate AFM modulations with  $\vec{q}_{\text{inc}} \parallel [110]$  and  $\vec{q}_{\text{inc}} \parallel [\bar{1}\bar{1}0]$  are degenerate for the magnetic field along [100] direction. Taking the coupling of the magnetic phase and the FFLO modulation of the superconducting phase into account we show that there could be multiple AFM phases in the  $H$ - $T$  phase diagram. The so-called "single- $q$ " phase corresponding to one of the two incommensurate wave vectors  $\vec{q}_{\text{inc}}$  is dominant in the phase diagram. However, the "double- $q$ " phase superposing both wave vectors can be induced under certain conditions, if there is commensuration condition between FFLO and AFM modulations. This phase is unstable against the second order transition towards a single- $q$  state as our Ginzburg-Landau model demonstrates.

We have shown that the single- $q$  phase is consistent with the experimental results of the NMR and neutron scattering measurements by taking into account the domain structure of two degenerate single- $q$  phases. A future experiment by the ultrasonic measurement has been discussed.

Finally, we discuss the field orientation dependence of the AFM order in CeCoIn<sub>5</sub>. Since the staggered magnetic moment lies along the  $c$ -axis owing to the spin-orbit coupling, the AFM order should be suppressed by the magnetic field along [001] direction. Furthermore, a small  $H_{c2}$  along  $c$ -axis indicates a weak paramagnetic effect which is unfavorable for the magnetic order.<sup>31,32)</sup> Thus, it is expected that the AFM order does not occur for this field direction even when the FFLO superconducting state is stabilized. Indeed, recent experiments have shown that the magnetic order is suppressed for  $\vec{H} \parallel [001]$ .<sup>49,50)</sup>

## Acknowledgements

The authors are grateful to D. Aoki, D. F. Agterberg, J. P. Brison, N. J. Curro, J. Flouquet, S. Gerber, R. Ikeda, M. Kenzelmann, G. Knebel, K. Kumagai, K. Machida, Y. Matsuda, V. F. Mitrović, K. Mitsumoto, and H. Tsunetsugu for fruitful discussions. This work was supported by a Grant-in-Aid for Scientific Research on Innovative Areas "Heavy Electrons" (No. 21102506) from

MEXT, Japan. It was also supported by a Grant-in-Aid for Young Scientists (B) (No. 20740187) from JSPS. Numerical computation in this work was carried out at the Yukawa Institute Computer Facility. YY is grateful for the hospitality of the Pauli Center of ETH Zurich. This work was also supported by the Swiss Nationalfonds and the NCCR MaNEP.

- 1) P. Fulde and R. A. Ferrell: Phys. Rev. **135** (1964) A550.
- 2) A. I. Larkin and Y. N. Ovchinnikov: Sov. Phys. JETP **20** (1965) 762.
- 3) H. A. Radovan, N. A. Fortune, T. P. Murphy, S. T. Hannahs, E. C. Palm, S. W. Tozer, and D. Hall: Nature **425** (2003) 51.
- 4) A. Bianchi, R. Movshovich, C. Capan, P. G. Pagliuso, and J. L. Sarrao: Phys. Rev. Lett. **91** (2003) 187004.
- 5) S. Uji, T. Terashima, M. Nishimura, Y. Takahide, T. Konoike, K. Enomoto, H. Cui, H. Kobayashi, A. Kobayashi, H. Tanaka, M. Tokumoto, E. S. Choi, T. Tokumoto, D. Graf, and J. S. Brooks: Phys. Rev. Lett. **97** (2006) 157001.
- 6) J. Singleton, J. A. Symington, M.-S. Nam, A. Ardavan, M. Kurmoo, and P. Day: J. Phys.: Condens. Matter **12** (2000) L641.
- 7) R. Lortz, Y. Wang, A. Demuer, P. H. M. Böttger, B. Bergk, G. Zwirner, Y. Nakazawa, and J. Wosnitza: Phys. Rev. Lett. **99** (2007) 187002.
- 8) J. Shinagawa, Y. Kurosaki, F. Zhang, C. Parker, S. E. Brown, D. Jérôme, J. B. Christensen, and K. Bechgaard: Phys. Rev. Lett. **98** (2007) 147002.
- 9) S. Yonezawa, S. Kusaba, Y. Maeno, P. Auban-Senzier, C. Pasquier, K. Bechgaard, and D. Jérôme: Phys. Rev. Lett. **100** (2008) 117002. Recent specific heat study by authors indicates that a possible FFLO phase is not stabilized in the bulk.
- 10) G. B. Partridge, W. Li, R. I. Kamar, Y.-A. Liao, and R. G. Hulet: Science **311** (2006) 503.
- 11) M. W. Zwierlein, A. Schirotzek, C. H. Schunck, and W. Ketterle: Science **311** (2006) 492.
- 12) Y. A. Liao, A. S. C. Rittner, T. Paprotta, W. Li, G. B. Partridge, R. G. Hulet, S. K. Baur, and E. J. Mueller: Nature **467** (2010) 567.
- 13) R. Casalbuoni and G. Nardulli: Rev. Mod. Phys. **76** (2004) 263.
- 14) Y. Matsuda and H. Shimahara: J. Phys. Soc. Jpn. **76** (2007) 051005.
- 15) T. Watanabe, Y. Kasahara, K. Izawa, T. Sakakibara, Y. Matsuda, C. J. van der Beek, T. Hanaguri, H. Shishido, R. Settai, and Y. Onuki: Phys. Rev. B **70** (2004) 020506.
- 16) C. Capan, A. Bianchi, R. Movshovich, A. D. Christianson, A. Malinowski, M. F. Hundley, A. Lacerda, P. G. Pagliuso, and J. L. Sarrao: Phys. Rev. B **70** (2004) 134513.
- 17) C. Martin, C. C. Agosta, S. W. Tozer, H. A. Radovan, E. C. Palm, T. P. Murphy, and J. L. Sarrao: Phys. Rev. B **71** (2005) 020503.
- 18) V. F. Mitrović, M. Horvatić, C. Berthier, G. Knebel, G. Laperot, and J. Flouquet: Phys. Rev. Lett. **97** (2006) 117002.
- 19) C. F. Miclea, M. Nicklas, D. Parker, K. Maki, J. L. Sarrao, J. D. Thompson, G. Sparn, and F. Steglich: Phys. Rev. Lett. **96** (2006) 117001.
- 20) V. F. Correa, T. P. Murphy, C. Martin, K. M. Purcell, E. C. Palm, G. M. Schmiedeshoff, J. C. Cooley, and S. W. Tozer: Phys. Rev. Lett. **98** (2007) 087001.
- 21) H. Adachi and R. Ikeda: Phys. Rev. B **68** (2003) 184510.
- 22) R. Ikeda: Phys. Rev. B **76** (2007) 134504.
- 23) R. Ikeda: Phys. Rev. B **76** (2007) 054517.
- 24) B.-L. Young, R. R. Urbano, N. J. Curro, J. D. Thompson, J. L. Sarrao, A. B. Vorontsov, and M. J. Graf: Phys. Rev. Lett. **98** (2007) 036402.
- 25) M. Kenzelmann, T. Strassle, C. Niedermayer, M. Sigrist, B. Padmanabhan, M. Zolliker, A. D. Bianchi, R. Movshovich, E. D. Bauer, J. L. Sarrao, and J. D. Thompson: Science **321** (2008) 1652.

- 26) M. Kenzelmann, S. Gerber, N. Egetenmeyer, J. L. Gavilano, T. Strässle, A. D. Bianchi, E. Ressouche, R. Movshovich, E. D. Bauer, J. L. Sarrao, and J. D. Thompson: *Phys. Rev. Lett.* **104** (2010) 127001.
- 27) Special Topics “Frontiers of Novel Superconductivity in Heavy Fermion Compounds”, *J. Phys. Soc. Jpn.* **76** (2007) No. 5.
- 28) Y. Yanase and M. Sigrist: *J. Phys.: Conf. Ser.* **150** (2009) 052287.
- 29) Y. Yanase and M. Sigrist: *J. Phys. Soc. Jpn.* **78** (2009) 114715.
- 30) K. Miyake: *J. Phys. Soc. Jpn.* **77** (2008) 123703.
- 31) R. Ikeda, Y. Hatakeyama, and K. Aoyama: *Phys. Rev. B* **82** (2010) 060510.
- 32) K. M. Suzuki, M. Ichioka, and K. Machida: arXiv:1009.2821.
- 33) Y. Kato, C. D. Batista, and I. Vekhter: arXiv:1104.0391
- 34) A. Aperis, G. Varelogiannis, P. B. Littlewood, and B. D. Simons: *J. Phys.: Condens. Matter* **20** (2008) 434235.
- 35) A. Aperis, G. Varelogiannis, and P. B. Littlewood: *Phys. Rev. Lett.* **104** (2010) 216403.
- 36) D. F. Agterberg, M. Sigrist, and H. Tsunetsugu: *Phys. Rev. Lett.* **102** (2009) 207004.
- 37) J. Paglione, M. A. Tanatar, D. G. Hawthorn, E. Boaknin, R. W. Hill, F. Ronning, M. Sutherland, L. Taillefer, C. Petrovic, and P. C. Canfield: *Phys. Rev. Lett.* **91** (2003) 246405.
- 38) A. Bianchi, R. Movshovich, I. Vekhter, P. G. Pagliuso, and J. L. Sarrao: *Phys. Rev. Lett.* **91** (2003) 257001.
- 39) F. Ronning, C. Capan, A. Bianchi, R. Movshovich, A. Lacerda, M. F. Hundley, J. D. Thompson, P. G. Pagliuso, and J. L. Sarrao: *Phys. Rev. B* **71** (2005) 104528.
- 40) K. Izawa, K. Behnia, Y. Matsuda, H. Shishido, R. Settai, Y. Onuki, and J. Flouquet: *Phys. Rev. Lett.* **99** (2007) 147005.
- 41) J. Panarin, S. Raymond, G. Lapertot, and J. Flouquet: *J. Phys. Soc. Jpn.* **78** (2009) 113706.
- 42) Y. Yanase and M. Sigrist: *J. Phys.: Condens. Matter* **23** (2010) 094219.
- 43) Y. Yanase and M. Sigrist: To appear in *J. Phys. Soc. Jpn. Suppl.*
- 44) N. J. Curro, B.-L. Young, R. R. Urbano, and M. J. Graf: arXiv:0908.0565; arXiv:0910.0288 (2009).
- 45) G. Koutroulakis, V. F. Mitrović, M. Horvatić, C. Berthier, G. Lapertot, and J. Flouquet: *Phys. Rev. Lett.* **101** (2008) 047004.
- 46) G. Koutroulakis, M. D. Stewart, V. F. Mitrović, M. Horvatić, C. Berthier, G. Lapertot, and J. Flouquet: *Phys. Rev. Lett.* **104** (2010) 087001.
- 47) K. Kumagai, H. Shishido, T. Shibauchi, and Y. Matsuda: *Phys. Rev. Lett.* **106** (2011) 137004.
- 48) M. Akatsu, T. Goto, Y. Nemoto, O. Suzuki, S. Nakamura, and S. Kunii: *J. Phys. Soc. Jpn.* **72** (2003) 205.
- 49) E. Blackburn, P. Das, M. R. Eskildsen, E. M. Forgan, M. Laver, C. Niedermayer, C. Petrovic, and J. S. White: *Phys. Rev. Lett.* **105** (2010) 187001.
- 50) C. Paulsen, D. Aoki, G. Knebel, and J. Flouquet: arXiv:1102.2703.